Physica C: Superconductivity and its applications 585 (2021) 1353870

Contents lists available at ScienceDirect

Physica C: Superconductivity and its applications

journal homepage: www.elsevier.com/locate/physc

Enhancing Transport Performance in 7-filamentary $Ba_{0.6}K_{0.4}Fe_2As_2$ Wires and Tapes via Hot Isostatic Pressing

Shifa Liu [a,b], Chao Yao [a], He Huang [a], Chiheng Dong [a], Wenwen Guo [a,b], Zhe Cheng [a,b], Yanchang Zhu [a], Satoshi Awaji [c], Yanwei Ma [a,b,*]

[a] Key Laboratory of Applied Superconductivity, Institute of Electrical Engineering, Chinese Academy of Sciences, Beijing 100190, China
[b] University of Chinese Academy of Sciences, Beijing 100049, China
[c] High Field Laboratory for Superconducting Materials, Institute for Materials Research, Tohoku University, Sendai 980-8577, Japan

ARTICLE INFO

Keywords:
Iron-based superconductors
$Ba_{0.6}K_{0.4}Fe_2As_2$
Multi-filamentary wires and tapes
Hot isostatic pressing
Mass density

ABSTRACT

Iron-based superconductors (IBS) are considered as potential materials for manufacturing high-field magnets, for which developing multi-filamentary conductors with high performance and high strength is essential. Herein, 7-filamentary Cu/Ag composite sheathed $Ba_{0.6}K_{0.4}Fe_2As_2$ (Ba122) round wires and tapes were successfully prepared through the *ex situ* powder-in-tube (PIT) method and treated by hot isostatic pressing (HIP) process. Pure Ba122 phase with roughly homogeneous element distribution was obtained in the superconducting filaments. The wires and tapes show very small low-temperature normal-state resistivity of 0.12 μΩ cm and 0.17 μΩ cm respectively owing to the high electrical conductivity of copper and silver. The HIP process greatly enhances the mass density of the superconducting filaments and promotes the formation of well-grown plate-like Ba122 grains. Vickers hardness measurements on the cross sections of these filaments reveal a rather good uniformity of the mass density. The transport critical current density (J_c) in the 7-filamentary Ba122/Ag/Cu round wires and tapes reached 1.3×10^4 A cm^{-2} and 4.8×10^4 A cm^{-2} at 4.2 K in 10 T respectively. These results indicate that hot isostatic pressing is advantageous in developing high-performance multi-filamentary iron-based superconductors.

1. Introduction

The discovery of iron-based superconductors inspired a new wave of high-temperature superconductivity research because of the new mechanism and their potential for practical applications [1,2]. Among numerous IBSs, the so-called 122-type iron pnictide superconductors, such as $Ba_{1-x}K_xFe_2As_2$ and $Sr_{1-x}K_xFe_2As_2$ (Sr122), display several outstanding characteristics that make them competitive candidates for high-field applications. They have modest transition temperatures T_c (up to 38 K), high upper critical fields H_{c2} and low anisotropy γ [3–6]. They also exhibit a distinct advantage over the cuprate superconductors that they have a less pronounced weak-link behavior of grain boundaries [7,8]. The feasibility of fabricating 122-type IBS wires and tapes with high-strength metals such as iron, copper and Monel alloy makes them quite appealing for high-field applications [9–11]. More importantly, they can be fabricated by a simple and low-cost PIT method, which is very conducive to mass production [12,13].

Despite all the above advantages, the key to practical applications is sufficiently high transport J_c. In the past decade, researchers have witnessed a substantial improvement in the current-carrying performance of IBS wires and tapes [14]. The highest transport J_c of 1.5×10^5 A cm^{-2} at 4.2 K in an applied magnetic field of 10 T was achieved by Huang *et al* in a hot-pressed silver-sheathed Ba122 tape [15]. In addition, some other researchers also reported achieving a transport J_c exceeding 10^5 A cm^{-2} at 4.2 K in 10 T in IBS tapes [16–18]. These excellent results suggest that IBSs are of great potential to become a new type of practical superconductors. However, these high J_c values were all achieved in mono-filamentary tapes. From the perspective of practical applications, the desired configuration of IBSs is in multi-filamentary form in order to reduce the AC loss and enhance the current-carrying stability, particularly in the form of isotropic round wires because they can be easily wound into coils or cabled into required shapes.

In term of sheath materials, silver is usually used as an inert barrier between high-strength metal sheath and the superconducting filaments in the fabrication of multi-filamentary 122-type IBSs, because it does not react with Ba122 or Sr122 phase. For example, Yao *et al* reported their

* Corresponding author. Key Laboratory of Applied Superconductivity, Institute of Electrical Engineering, Chinese Academy of Sciences, Beijing 100190, China
E-mail address: ywma@mail.iee.ac.cn (Y. Ma).

https://doi.org/10.1016/j.physc.2021.1353870
Received 1 February 2021; Received in revised form 28 February 2021; Accepted 8 April 2021
Available online 16 April 2021

systematic work on the fabrication of 7-, 19- and 114-filamentary Sr-122/Ag/Fe tapes, achieving J_c values of 1.4 × 10^4, 8.4 × 10^3 and 6.3 × 10^3 A cm^{-2} at 4.2 K and 10 T respectively [9,19]. They also prepared high strength 7-filamentary Sr122/Ag/Monel tapes, showing almost no J_c degradation under a compressive strain of 0.6% [11]. When choosing the outer sheath materials, another issue that needs to be considered is the thermal conductivity and stability of the iron-pnictide conductors. As proposed by Dong *et al*, copper is an ideal metal due to its high electrical and thermal conductivity [20].

Recently the HIP process has been demonstrated as a successful method to achieve high J_c in mono-filamentary 122-type IBS wires and tapes [21–24]. In spite of the many reported studies on the fabrication of multi-filamentary IBS tapes and wires, to the best of the authors' knowledge, no work concerning the preparation of multi-filamentary IBS wires and tapes through the HIP process has been reported. In this work, we applied the HIP process in the final heat treatment of the 7-filamentary Ba122/Ag/Cu round wires and tapes. The transport J_c of the as-obtained samples was evaluated and relevant characterizations were conducted to gain a comprehensive understanding of the role of the HIP process in the preparation of multi-filamentary Ba122 conductors.

2. Experimental section

The 7-filamentary Ba122/Ag/Cu round wires and tapes were prepared by an *ex situ* PIT method. The precursor of the Ba122 wires was prepared by a direct reaction of barium, potassium, iron, and arsenic at 900 °C for 35 h. Before the sintering, barium fillings, potassium pieces and iron and arsenic powders were mixed with the nominal composition of $Ba_{0.6}K_{0.46}Fe_2As_2$ and then fully ball-milled. The 15wt% excess potassium was added to compensate the high temperature loss. The precursor of the Ba122 tapes was prepared by a two-step method; see the reference for details [23]. The as-obtained precursors were ground using an agate mortar in an argon-filled glovebox and then packed into silver tubes. The silver tube for the 7-filamentary wires has an outer diameter (OD) of 8.0 mm and an inner diameter (ID) of 5.0 mm. A thinner-walled silver tube was utilized in the 7-filamentary tapes with an OD of 8.0 mm and an ID of 6.0 mm. The silver tubes were swaged and drawn into silver-sheathed wires with an OD of 1.33 mm. Then the silver wires were cut into short pieces in order to be restacked in copper tubes with an OD of 6.0 mm and an ID of 4.0 mm. After restacking, the copper tubes were again swaged and drawn into wires with an OD of 1.50 mm. The thin tapes were prepared by further flat rolling with a target thickness of 0.30 mm. Finally, the round wires and tapes were heat-treated under 150 MPa of pressure at 740 °C for 2 h and 1 h respectively.

The field-dependent transport critical current measurements were performed at High Field Laboratory for Superconducting Materials at Sendai, using the standard four-probe method along with a criterion of 1 μV cm^{-1}. Short pieces of the Ba122 wires and tapes were embedded in conductive resin and then polished for optical microscopic observation, Vickers hardness measurements and element mapping. The Vickers hardness was measured by the Wilson 402MVD tester with 0.025 kg load and 10 s duration. The temperature dependent resistance was evaluated by a Quantum Design Physical Property Measurement System (PPMS). The magnetic property was evaluated by a SQUID-VSM on a Quantum Design Magnetic Property Measurement System (MPMS). Chemical methods were utilized to remove the metal sheath away to acquire the Ba122 filaments. X-ray diffraction (XRD, Bruker D8 Advance) analysis and scanning electron microscopy (SEM, Zeiss SIGMA) observation were performed on these filaments. Using an electron probe micro-analyzer (EPMA, JEOL JXA8320), the element distribution of the 7-filamentary round wires and tapes was characterized on their well-polished cross sections.

3. Results and discussion

3.1. Seven-filamentary Ba122/Ag/Cu wires

First of all, the in-field transport J_c of the 7-filamentary Ba122/Ag/Cu round wires was evaluated at 4.2 K with an external magnetic field perpendicular to the wire axis, and the best results are shown in Fig. 1 (a). By the way, the specifications of the round wire were acquired with an optical microscope although not presented. The cross-sectional image of the wire can be found in Fig. 3. The transport J_c reached 1.3 × 10^4 A cm^{-2} at 4.2 K in 10 T, which is comparable to the reported J_c in the mono-filamentary Ba122 round wires [21,22]. Notably, it is more than an order of magnitude higher than the J_c in the 114-filamentary Sr122/Ag/Fe round wires [9]. A weak field dependence of the J_c in the wire was observed, showing the excellent high-field transport performance of Ba122. Actually, due to lack of texture in as-drawn 122-type iron-pnictide round wires, transport J_c in this type of conductors is almost an order of magnitude lower than that in the rolled tapes. Nevertheless, isotropic round wires are still the most desirable form of superconductors for high-field magnets. Based on the power law $E(I)/E_c=(I/I_c)^n$, where I is the transport current and E is the voltage drop across the sample, one can calculate the n-value, which represents the sharpness of the transition from superconducting state to normal state. Superconducting materials of high n-values tent to cause much less electrical and thermal dissipation in a magnet operated in persistent current mode, and are more favorable as the magnet materials. The calculated n-values for the 7-filamentary Ba122 wire at different magnetic fields are presented in Fig. 1(a). The n-values tent to be lower in relatively low magnetic fields, ~15 in 2 T and ~19 in 4 T. In fields from 6 T to 10 T, n-values range from 23-24, which are slightly lower than that of the silver-sheathed Sr122 tapes [25].

Fig. 1(b) presents the temperature dependent resistivity of the 7-filamentary Ba122/Ag/Cu round wire from 10 K to 300 K. The inset shows the resistivity transition in different magnetic fields. The field was applied vertical to the wire axis. The transition temperature T_c of the wire is 36.8 K in self-field and reduced to 35.6 K after applying a magnetic field of 0.5 T, which can be explained by the creep of vortices considering the very low resistance near the T_c [26]. Besides, the substantial magneto-resistance can be observed in the normal state as a consequence of the very low normal-state resistivity. A similar phenomenon was also observed in MgB_2 [27]. For designing superconducting magnets, the residual resistivity ratio (*RRR*) is an important parameter. Based on the ρ-T curve from 10 K to 300 K, the *RRR*, ρ_{300K}/ρ_{40K}, is calculated as about 18. The low-temperature normal-state resistivity (40 K) is very small, about 0.12 μΩ cm. These features are advantageous because magnets made from these wires are less likely to quench.

The phase composition of the 7-filamentary Ba122/Ag/Cu round wire was investigated through XRD analysis, which was performed by placing the seven Ba122 filaments side by side. As shown in Fig. 1(c), Ba122 is the main phase inside the wire. Except for silver and unreacted iron, no other impurities were detected. Additionally, the XRD pattern of the round wire is quite similar to that of the randomly orientated precursor powder, that is, the (103) peak has the strongest intensity and (00*l*) peaks have low intensity, indicating that the Ba122 grains in the wire are probably randomly orientated [23].

Fig. 2(a) shows the diamagnetic transition of the wire, which was measured in the field-cooled (FC) and zero-field-cooled (ZFC) processes. The magnetic field is perpendicular to the wire axis. The ZFC curve shows a sharp transition with the onset temperature T_c=36.3 K. Fig. 2(b) presents the magnetization hysteresis loops of the round wire. No trace of the fishtail effect was found in the temperatures ranging from 4.2 K to 30 K, which is different from what was observed in the $Ba_{0.6}K_{0.4}Fe_2As_2$ single crystals [28]. The inset presents the difference of the magnetization values between the upper and lower branches of the hysteresis loops. It shows that an external magnetic field of 7 T is not sufficient to

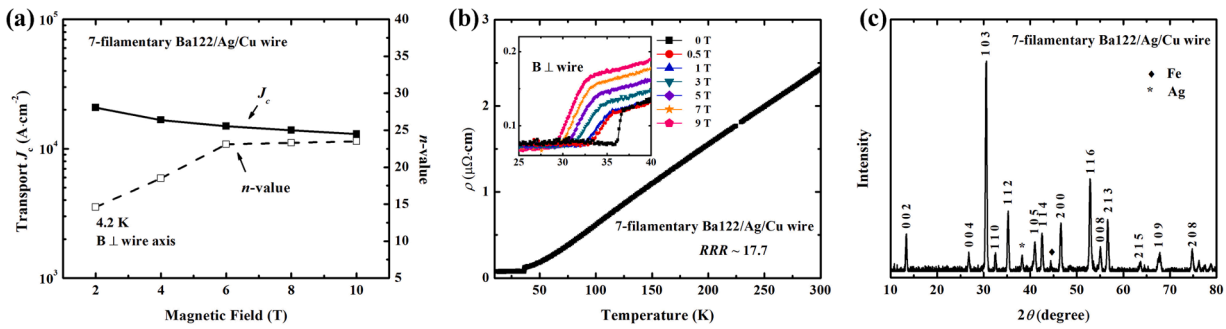

Fig. 1. (a) Transport J_c and n-values as a function of the applied magnetic fields for the 7-filamentary Ba122/Ag/Cu wire at 4.2 K. (b) Resistivity of the wire at temperatures from 10 K to 300 K. The inset shows the low-temperature resistivity at different magnetic fields from 0 T to 9 T. (c) XRD pattern measured on the filaments of the 7-filamentary Ba122/Ag/Cu wire.

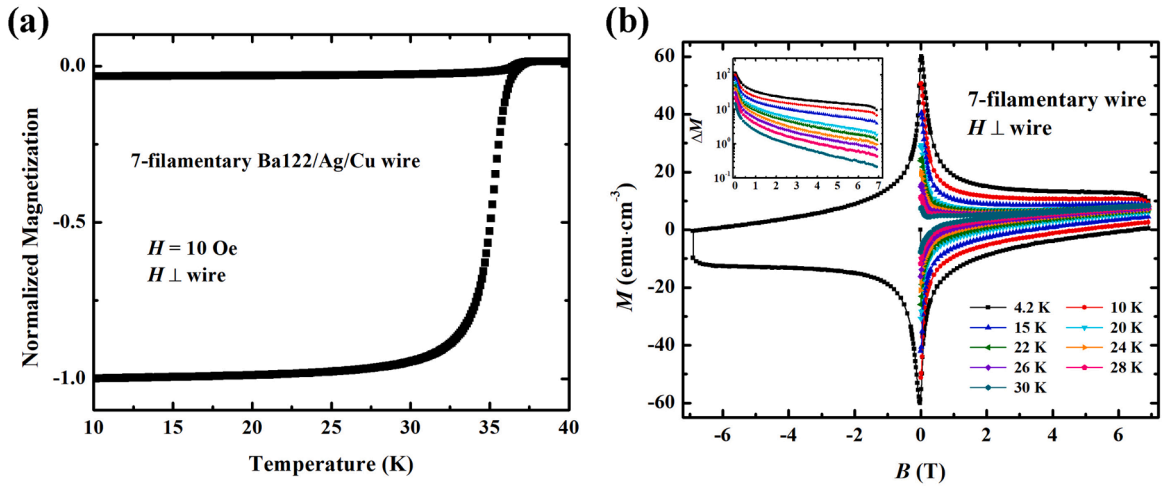

Fig. 2. (a) Normalized magnetization of the 7-filamentary Ba122/Ag/Cu wire versus temperatures measured in the ZFC and FC procedures. (b) The magnetization hysteresis loops of the wire measured at temperatures from 4.2 K to 30 K. The inset shows the difference of the magnetization values between the upper and lower branches of the loops.

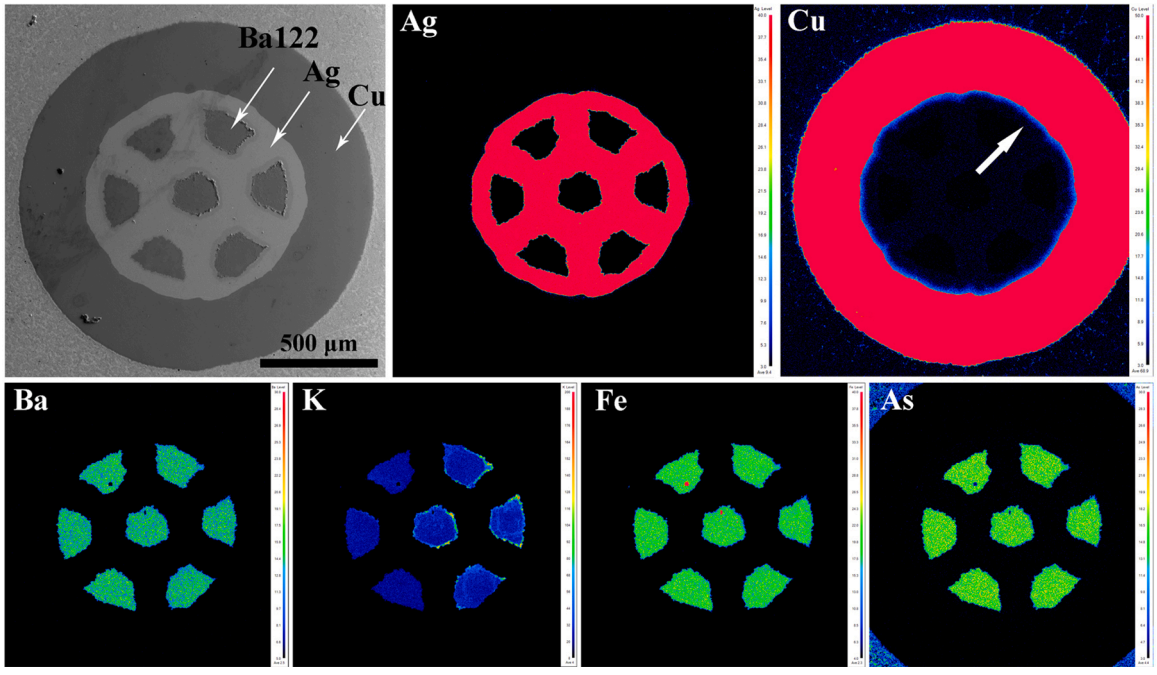

Fig. 3. SE image of the cross section of the 7-filamentary Ba122/Ag/Cu wire and element distribution maps on the cross section.

achieve the closure of the hysteresis loop even at 30 K, which suggests that the round wire has a high irreversibility field.

The homogeneity of the element distribution in the wire was investigated through the EPMA technique, as shown in Fig. 3. A secondary electron (SE) image of the cross section is also presented. Clear boundaries between the silver matrix and the superconducting filaments can be seen and the filaments are symmetrically distributed. These mapping images of barium, iron and arsenic demonstrate a roughly homogenous distribution. As for the map of potassium, it needs to be clarified that the inhomogeneity of potassium is not intrinsic to the filaments because an unknown reaction occurred on the surface of the filaments after the polishing, which can also be observed in the SE image. Several iron-rich dots were also detected, which is in consistent with the XRD results. Unfortunately, evidence of copper diffusing into silver matrix was also found, as indicted by the white arrow in the map of copper. According to Dong *et al*, this may cause a deterioration of thermal conductivity and needs more attention [20].

Fig. 4(a) shows a typical cross sectional image of a filament in the 7-filamentary Ba122/Ag/Cu round wire viewed by SEM, and Fig. 4(b) presents a partial enlarged view of its central region. As can be seen, Ba122 grains in the wire are well-grown, plate-like but randomly orientated, and the filament is dense. For iron-pnictide superconductors, the mass density of the superconducting cores can be evaluated via Vickers hardness (*Hv*). High *Hv* indicates a dense iron-pnictide phase and consequently is beneficial to the transport performance. To show the density variation between filaments, detailed *Hv* measurements were performed on the well-polished cross section of the 7-filamentary wire. Fig. 5(a) shows the average *Hv* values of these filaments and their respective standard deviations, in which filament #4 refers to the one in the center of the wire. All the seven filaments have an average *Hv* above 200 with a reasonably small *Hv* fluctuation. Fig. 5(b) presents the details of the *Hv* measurements on filament #4. The hardness testing sites distributed approximately equidistantly along the three lines indicated in the inset. The abscissa x is defined as the distance between the testing sites and the central position of the lines. A total of 14 points were tested, which were kept not too close to the edge of the filament. Similar measurements were also performed on the other six filaments. The *Hv* values in the wire are much higher than many other iron-pnictide tapes [9,29,30], indicating great improvement on the grain connectivity was achieved through the HIP densification process. Good grain connectivity in the HIP-sintered wire is considered to be one of the main reasons for the high transport properties.

3.2. Seven-filamentary Ba122/Ag/Cu tapes

In the preparation of the 7-filamentary Ba122/Ag/Cu tapes, a thinner-walled silver tube was utilized in order to increase to the filling factor and reduce the consumption of silver. This is important because increasing the filling factor can improve the current carrying capacity of the conductors and reducing the silver consumption can greatly cut down the fabrication cost. The calculated filling factor for the tape is 16.0% and the proportion of silver is 21.6%. A typical cross section of the tape can be found in Fig. 8. The silver matrix remains intact even though a thin-walled silver tube was utilized. The filaments in the tape are all elongated, which is quite different from the short-rod-shaped cores in the Monel- or iron-sheathed Sr122 tapes [9,11]. This can be attributed to a much improved deformation of the superconducting cores resulted from the good workability of copper and relatively smaller tape thickness. As a result, relatively high degree of texture is expected in the copper-sheathed 7-filamentary tapes. Due to the intrinsic weak-linked grain boundaries in 122-type IBSs, texture in the filaments is beneficial to their transport properties.

Fig. 6(a) shows the highest field-dependent transport J_c of the 7-filamentary Ba122 tapes measured at 4.2 K with the external magnetic field parallel to the tape surface. The calculated *n*-values are also presented. High J_c of 7.1 $\times$ 10^4 A cm^{-2} in 2 T and 4.8 $\times$ 10^4 A cm^{-2} in 10 T were achieved, showing very weak field dependence. The calculated *n*-values range from 27 to 29 and are comparable to the reported values of the Sr122 tapes [11,25]. Fig. 6(b) presents the temperature dependent resistivity of the 7-filamentary Ba122 tape in various magnetic fields. The field was applied vertical to the tape surface. The transition temperature T_c for the tape is 37.3 K and the calculated *RRR* (ρ_{300K}/ρ_{40K}) is about 21. The low-temperature normal-state resistivity (40 K) is 0.17 μΩ cm, close to that of the 7-filamentary Ba122 round wire above, because the resistivity in normal state is mainly contributed by copper and silver. Excellent conductivity of copper makes it advantageous as a sheath material. The inset presents the resistivity transition in different magnetic fields, in which a large reduction of T_c after applying a magnetic field of 0.5 T and the magneto-resistance were also observed. The phase purity and texture of the 7-filamentary Ba122/Ag/Cu tape was studied by performing XRD test on the surfaces of the bare Ba122 filaments. Fig. 6(c) shows the XRD patterns acquired on the surface of two different filaments in the tape. Ba122 phase is dominant in these filaments with unreacted iron being detected. The relative intensities of the (00*l*) peaks with respect to that of the (103) peak are significantly increased, indicating that c-axis texture was induced in the tape via the flat-rolling, which are favorable to the transport properties. However, the XRD patterns also reveal a clear difference of the degree of texture between filaments, indicating a deformation variation between different filaments in the tape.

Fig. 7(a) shows the diamagnetic transition of the 7-filamentary Ba122 tape measured in the FC and ZFC processes with the magnetic field perpendicular to the tape surface. The ZFC curve shows a relatively smooth transition compared to that of the round wire with an onset temperature T_c=36.7 K. This is probably due to relatively uneven performance in the 7-filamentary tape compared to the round wire, given that an additional rolling process was applied. The magnetization hysteresis loops were also presented in Fig. 7(b) with the inset presenting the differences between the upper and lower branches. The hysteresis loop of the tape is also not closed in an external magnetic field of 7 T at

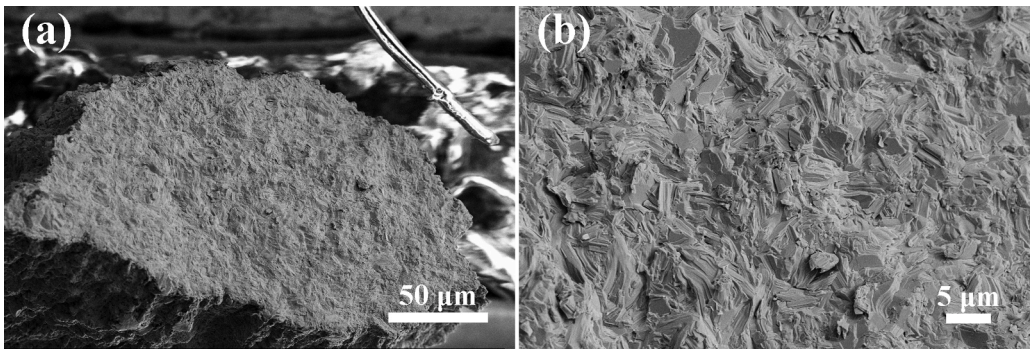

Fig. 4. (a) Typical SEM cross-sectional view of a filament in the 7-filamentary Ba122/Ag/Cu wire and (b) partially enlarged view of the region in the center.

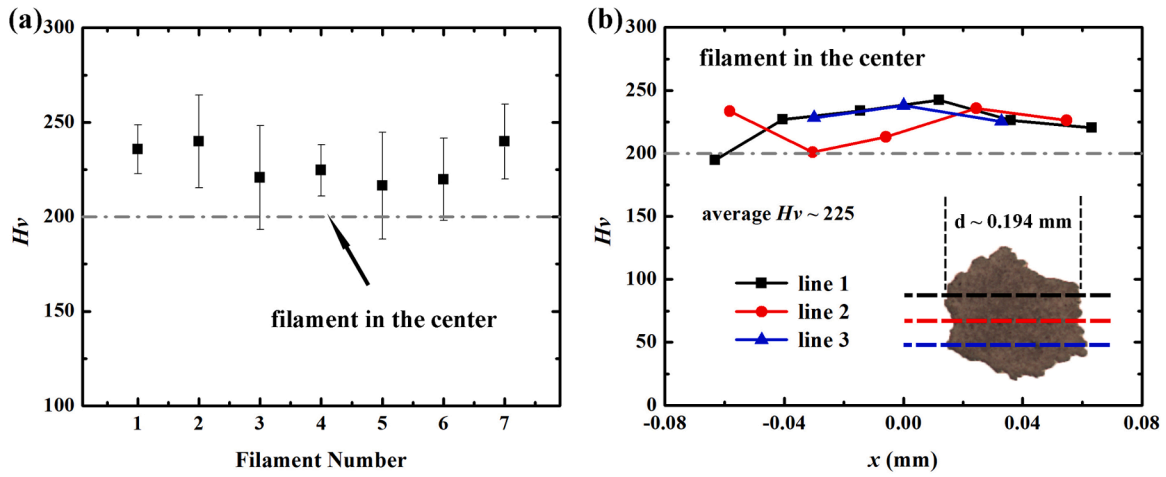

Fig. 5. (a) Average *Hv* values and the corresponding standard deviations of the filaments in 7-filamentary Ba122/Ag/Cu wire. Filament #4 is the one in the center of the wire. (b) Details of the *Hv* measurements on filament #4.

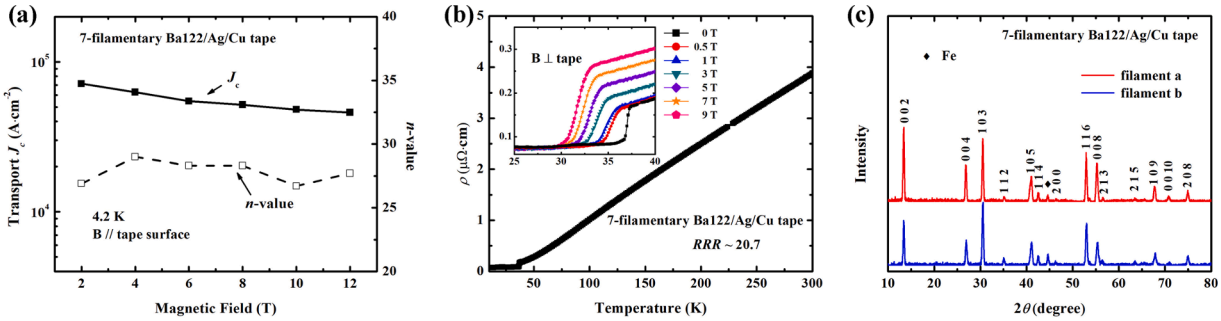

Fig. 6. (a) Transport J_c and *n*-values as a function of the applied magnetic fields for the 7-filamentary Ba122/Ag/Cu tape at 4.2 K. (b) Resistivity of the tape at temperatures from 10 K to 300 K. The inset shows the low-temperature resistivity at different magnetic fields from 0 T to 9 T. (c) XRD pattern measured on the surfaces of two different Ba122 filaments of the 7-filamentary Ba122/Ag/Cu tape.

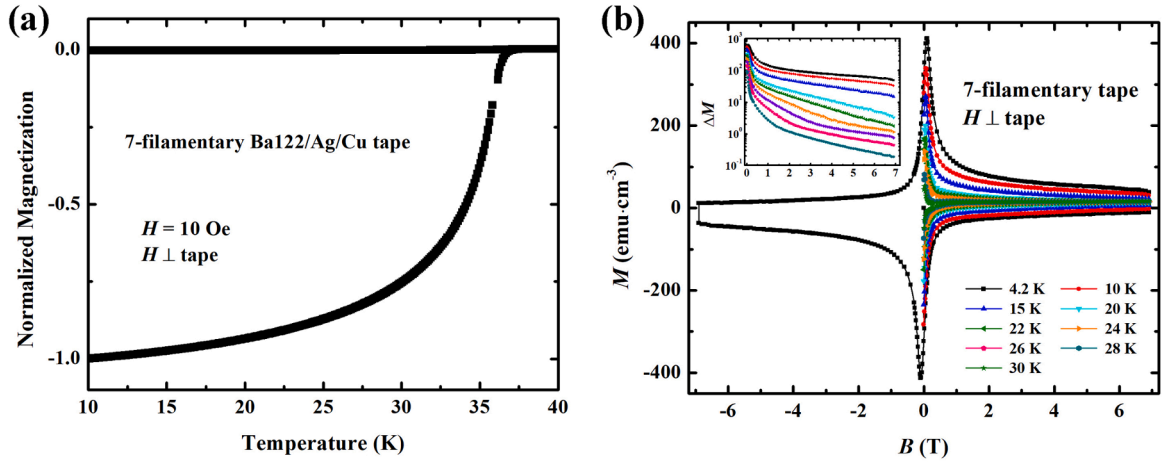

Fig. 7. (a) Normalized magnetization of the 7-filamentary Ba122/Ag/Cu tape versus temperatures measured in the ZFC and FC procedures. (b) The magnetization hysteresis loops of the tape measured at temperatures from 4.2 K to 30 K. The inset shows the difference of the magnetization values between the upper and lower branches of the loops.

30 K, suggesting that Ba122 phase intrinsically has a high irreversibility field.

Fig. 8 presents the element distribution mapping images on the cross sections of the 7-filamentary Ba122/Ag/Cu tape. The measurement was performed on the entire cross section of the tape, showing the overall distribution of each element in the sample. Except for the potassium, the distribution of barium, iron and arsenic is roughly uniform. Tiny iron-rich dots were observed, showing that unreacted iron exists. The silver layer is intact and has a clear boundary with the Ba122 phase. In the map of copper, it was found that a small amount of copper diffused into the silver layer, the same as the round wires.

Fig. 9(a) shows the SEM cross-sectional views of a Ba122 filament in

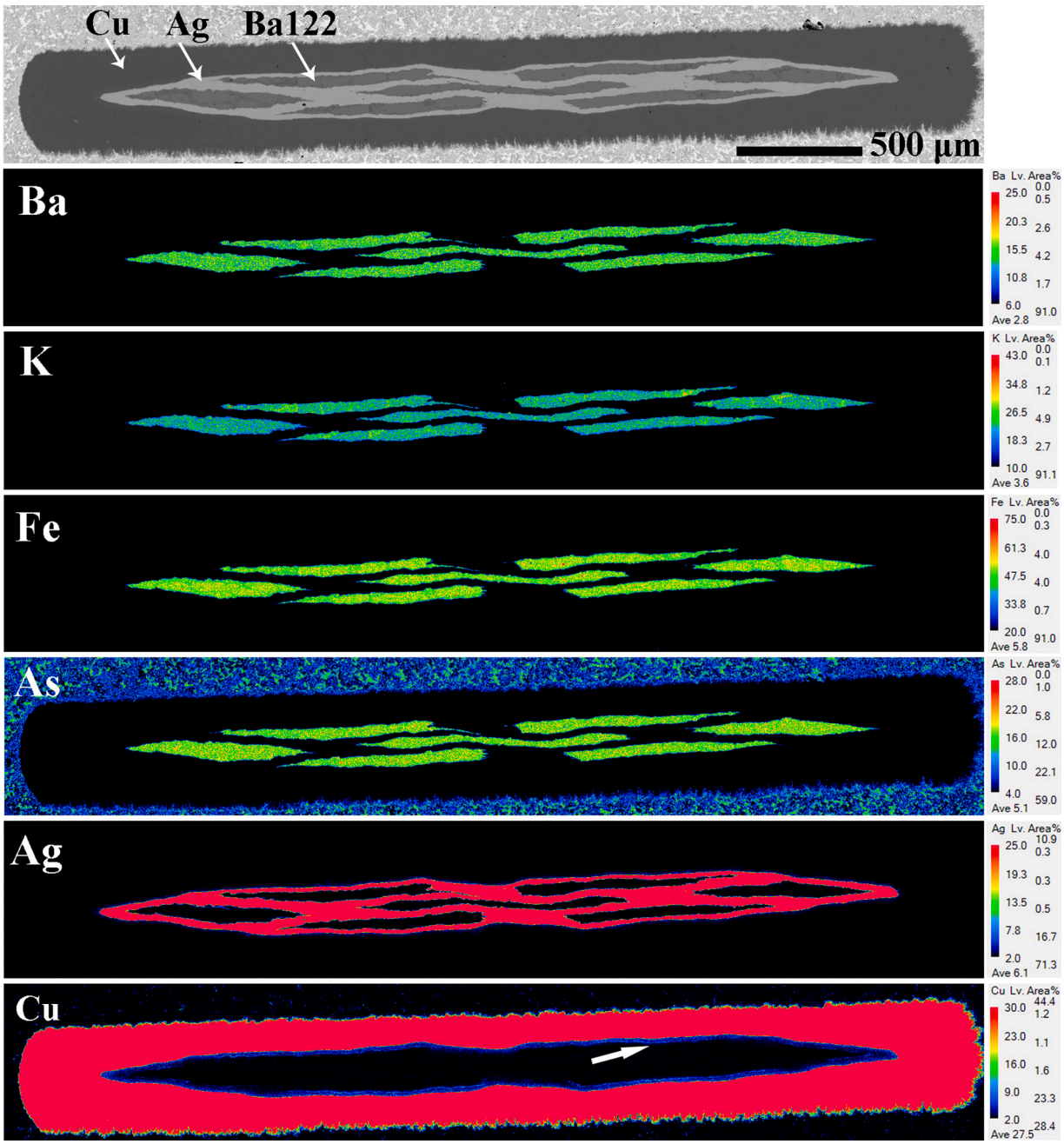

Fig. 8. SE image of the cross section of the 7-filamentary Ba122/Ag/Cu tape and element distribution maps on the cross section.

the 7-filamentary Ba122 tape with a maximum thickness of 48 μm. Fig. 9 (b) shows the SEM image of the central part and Fig. 9(c) shows a partial enlarged view. Typical microstructure of HIP-sintered Ba122 tapes can be observed, that is, well-grown plate-like grains aligned roughly parallel to the tape surface. The mass density of the filaments in the 7-filamentary Ba122 tape was also evaluated by the *Hv* measurements. Fig. 10 (a) shows the average *Hv* values and the corresponding standard deviations of these filaments. Filament #4 refers to the filament in the center. The average *Hv* values are 226, 236, 229, 209, 238, 240 and 239 for the seven filaments in the tape, which are very high values. Small *Hv* fluctuations were also found in these filaments. Besides, it can be seen that the filament in the center has a relatively lower average *Hv*, indicating degradation of the mass density occurred in the center of the tape. Fig. 10(b) shows the *Hv* distribution of filament #2 and filament #4. The measurements were conducted along the long side of the cross sections of the filaments. For each position, the testing site was located in the middle due to the limited thickness of the filaments. Therefore, it should be pointed out that the *Hv* values mainly reflect the mass density of the middle part of the filaments. Nevertheless, the high density and good uniformity of these filaments exhibit the huge advantages of HIP process in the densification of superconducting cores.

3.3. Discussion

For IBSs aiming at practical applications, research on the preparation of multi-filamentary conductors is inevitable. To boost their potential, low-cost high-strength metals are the desired sheath materials. Prior to this work, there have been several reports focusing on the fabrication of iron- and Monel-sheathed multi-filamentary Sr122 wires and tapes. However, since these metals are too strong to be deformed, the cross-sectional images of the final tapes show poor deformation of the superconducting filaments. The cross sections of the filaments are short-

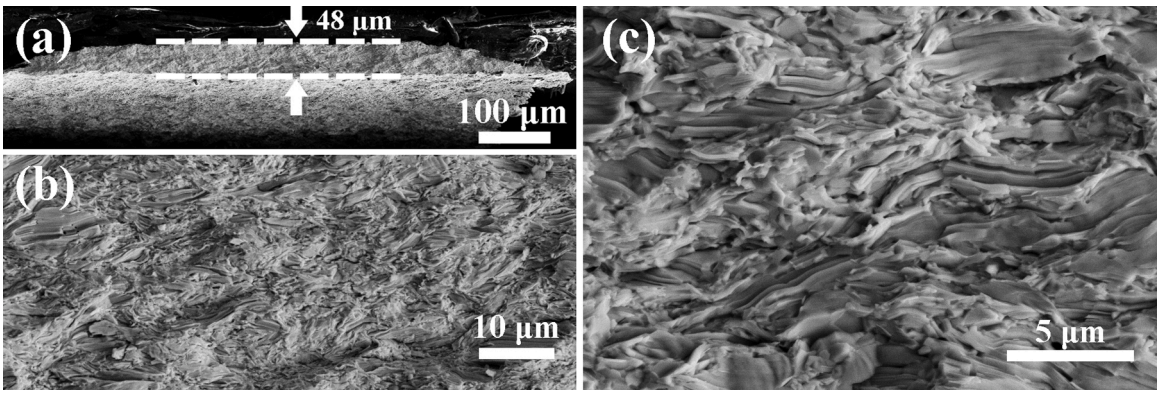

Fig. 9. (a) Typical SEM cross-sectional images of a filament in the 7-filamentary Ba122/Ag/Cu tape with a maximum thickness of 48 μm. (b) SEM image of the region in the center of the filament and (c) a partially enlarged view.

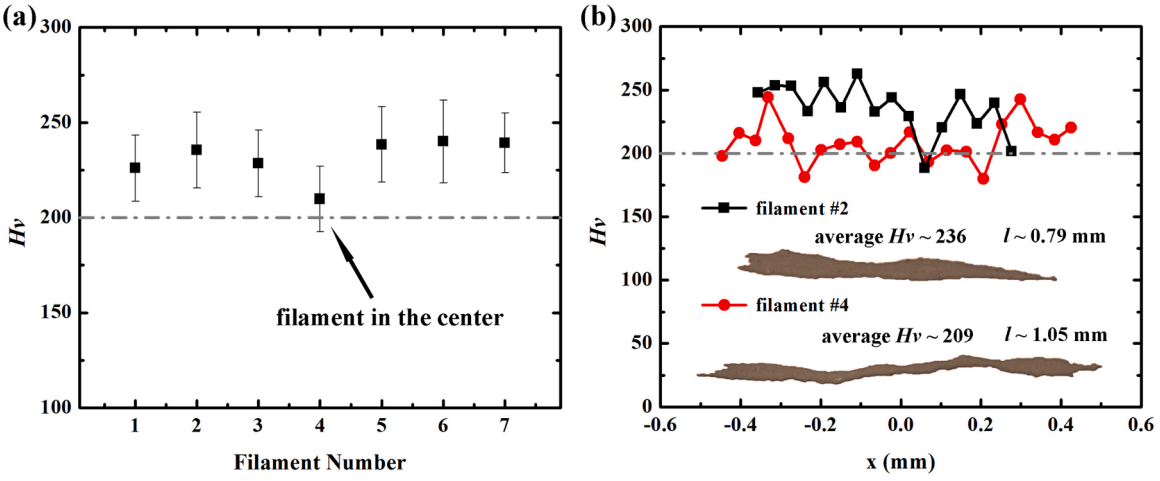

Fig. 10. (a) Average *Hv* values and the corresponding standard deviations of the filaments in 7-filamentary Ba122/Ag/Cu tape. Filament #4 is the one in the center of the tape. (b) Details of the *Hv* measurements on filament #2 and #4.

rod-shaped and the ones in the center are usually broken. In addition, the grains in these samples appear to be not well-grown and their hardness *Hv* values are also not sufficiently high. To overcome these issues, multi-filamentary Ba122/Ag/Cu round wires and tapes were prepared and treated by the HIP process.

We performed detailed *Hv* measurements on the well-polished cross sections of the HIP-sintered 7-filamentary Ba122 round wire and tape in purpose of investigating the influence of the HIP process on the mass density of these filaments. Actually, the mass density of an IBS conductor prepared by the *ex situ* PIT method is usually not 100%, which means that part of the space inside the metal sheath is filled with gas, in this case argon. During the high-temperature sintering, the gas expands and agglomerates into holes, which will definitely de-densify the superconducting filaments and consequently cause J_c degradation in these samples. Given that the HIP process has been proved effective in suppressing the de-densificationin mono-filamentary IBS tapes and wires, we further prove its effectiveness in the multi-filamentary iron-pnictide conductors. The *Hv* values of the filaments in both 7-filamentary Ba122 round wire and tape are very high, indicating a high mass density in these filaments. The microstructure in these filaments was also observed, showing that dense filaments with well-grown plate-like Ba122 grains were formed during the HIP treatment. To conclude, 7-filamentary Ba122/Ag/Cu round wire and tape with highly dense superconducting filaments were successfully fabricated.

Fig. 11 compares the transport J_c of the 7-filamentary Sr122/Ag/Fe and Sr122/Ag/Monel tapes sintered in ambient pressure with that of the 7-filamentary Ba122/Ag/Cu tape in this work. It can be seen that an enhancement in J_c of more than a factor of 3 in the 7-filamentary Ba122/Ag/Cu tape in 10 T was obtained compared to the 7-filamentary Sr122/

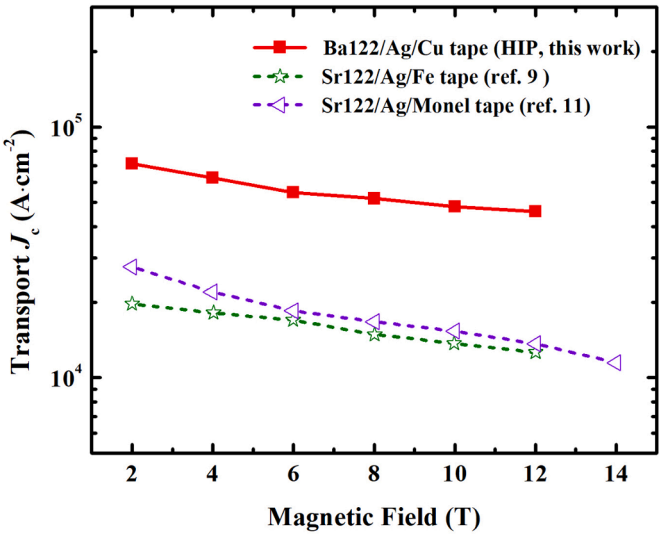

Fig. 11. Comparison of the J_c of the 7-filamentary Sr122/Ag/Fe and Sr122/Ag/Monel tapes with that of the 7-filamentary Ba122/Ag/Cu tape in this work.

Ag/Fe and Sr122/Ag/Monel tapes. Here we propose that the high transport performance in our tape is a result of multiple factors. Firstly, the entire conductor is deformed more uniformly due to the good workability of copper, and the filaments are elongated. Though there is no comparable reported data, the degree of texture in our tape is probably higher compared to the iron- or Monel-sheathed tapes. Secondly, well-grown plate-like Ba122 grains were achieved owing to the HIP densification process, as shown in Fig. 9. Besides, the mass density of the superconducting filaments was greatly increased as indicated by the *Hv* values. Thirdly, the pure Ba122 phase and roughly homogenous element distribution are beneficial for high performance. More importantly, in addition to J_c enhancement, copper is more favorable for manufacturing high-filed magnets due to its excellent electrical and thermal conductivity and non-magnetic nature. In a word, the HIP process and copper sheath are two preferred choices for developing multi-filamentary iron-pnictide superconductors.

Finally, it would be beneficial to have some words on the further improvement of the multi-filamentary Ba122 superconductors. Firstly, as revealed by both the XRD patterns and the EPMA images, excess iron exists in the final-sintered wires and tapes. Since there is not much research on the role of iron additions on the performance of IBSs, it cannot be arbitrarily considered as a J_c impediment. Secondly, the deformation of the filaments in the 7-filamentary tape is inhomogeneous, which leads to the variation of degree of texture in the tape, as shown in Fig. 6(c). Besides, relatively lower *Hv* values were found in the filament at the center of the 7-filamentary tape. These results indicates that the performance of different filaments in the tape may be uneven, which is also the reason for a relatively smooth magnetic transition in Fig. 7(a). For the optimization of deformation, numerical modelling of the deformation behavior of 122-type iron pnictide powder is urgently needed. The influence of the precursor powder, including its geometry and its particle size, on the deformation process needs to be addressed. Xu *et al* [30] recommended a bidirectional rolling process, which realized a rather uniform deformation of the superconducting filaments compared to the commonly used unidirectional rolling. Using silver alloy instead of silver as the inner sheath may also have a positive effect [31]. Thirdly, optimization in term of the proportion of silver in the conductors also matters. Though thin-walled silver tubes can reduce the costs, using excessively thin-walled silver tubes can lead to a broken silver barrier. All the above issues require plenty of optimization on the precursor preparation and the deformation process based on multi-filamentary samples.

4. Conclusions

In summary, we have fabricated 7-filamentary Ba122/Ag/Cu round wires and tapes through the PIT method and HIP process. High transport J_c of 1.3×10^4 A cm^{-2} and 4.8×10^4 A cm^{-2} at 4.2 K in 10 T were achieved respectively, which are the first reported J_c values for HIP-sintered multi-filamentary IBS tapes and wires. Both samples show high *n*-values, very small low-temperature normal-state resistivity with large *RRR* values and high irreversibility fields, which are favorable for manufacturing high-field magnets. Characterizations on the 7-filamentary round wires and tapes reveal that the high transport J_c was a result of multiple factors, including pure Ba122 phase, well-grown grains with the high core density and roughly uniform element distribution. Both samples have a high and rather uniform mass density, which shows the superiority of the HIP process in densifying the superconducting cores. In short, our work demonstrates that the HIP technique can be a good choice for developing multi-filamentary IBS round wires and tapes, and copper is an ideal sheath metal for IBSs.

CRediT authorship contribution statement

Shifa Liu: Validation, Formal analysis, Investigation, Writing – original draft. **Chao Yao:** Validation, Resources, Writing – review & editing, Project administration, Funding acquisition. **He Huang:** Investigation, Validation, Resources. **Chiheng Dong:** Investigation, Validation, Resources. **Wenwen Guo:** Investigation, Validation. **Zhe Cheng:** Investigation. **Yanchang Zhu:** Investigation. **Satoshi Awaji:** Resources. **Yanwei Ma:** Resources, Writing – review & editing, Supervision, Project administration, Funding acquisition.

Declaration of competing interest

The authors declare no competing financial interests or personal relationships that could have appeared to influence the work reported in this paper.

Acknowledgements

This work is supported by the National Key R&D Program of China (Grant Nos. 2018YFA0704200 and 2017YFE0129500), the National Natural Science Foundation of China (Grant Nos. 51861135311, U1832213 and 51721005), the Strategic Priority Research Program of Chinese Academy of Sciences (Grant No. XDB25000000) and the Key Research Program of Frontier Sciences of Chinese Academy of Sciences (Grant No. QYZDJ-SSW-JSC026).

References

[1] H Hosono, A Yamamoto, H Hiramatsu, Recent advances in iron-based superconductors toward applications, Mater Today 21 (3) (2018) 278–302.
[2] Z-A Ren, Z-X. Zhao, Research and Prospects of Iron-Based Superconductors, Adv Mater 21 (45) (2009) 4584–4592.
[3] M Rotter, M Tegel, D. Johrendt, Superconductivity at 38 K in the iron arsenide $(Ba_{1-x}K_x)Fe_2As_2$, Phys Rev Lett 101 (10) (2008), 107006.
[4] K Sasmal, B Lv, B Lorenz, Superconducting Fe-based compounds $(A_{1-x}Sr_x)Fe_2As_2$ with A=K and Cs with transition temperatures up to 37 K, Phys Rev Lett 101 (10) (2008), 107007.
[5] X-L Wang, SR Ghorbani, Very strong intrinsic flux pinning and vortex avalanches in (Ba, K)Fe_2As_2 superconducting single crystals, Phys Rev B 82 (2) (2010) 5626–5628.
[6] HQ Yuan, J Singleton, FF Balakirev, Nearly isotropic superconductivity in (Ba,K) Fe_2As_2, Nature 457 (7229) (2009) 565–568.
[7] H Sato, H Hiramatsu, T Kamiya, Enhanced critical-current in P-doped $BaFe_2As_2$ thin films on metal substrates arising from poorly aligned grain boundaries, Sci Rep 6 (1) (2016) 36828.
[8] T Katase, Y Ishimaru, A Tsukamoto, Advantageous grain boundaries in iron pnictide superconductors, Nat Commun 2 (2011) 409.
[9] C Yao, H Lin, Q Zhang, Critical current density and microstructure of iron sheathed multifilamentary $Sr_{1-x}K_xFe_2As_2$/Ag composite conductors, J Appl Phys 118 (20) (2015).
[10] H Lin, C Yao, H Zhang, Large transport J_c in Cu-sheathed $Sr_{0.6}K_{0.4}Fe_2As_2$ superconducting tape conductors, Sci Rep 5 (2015) 11506.
[11] C Yao, D Wang, H Huang, Transport critical current density of high-strength $Sr_{1-x}K_xFe_2As_2$/Ag/Monel composite conductors, Supercond Sci Technol 30 (7) (2017), 075010.
[12] Y. Ma, Progress in wire fabrication of iron-based superconductors, Supercond Sci Technol 25 (11) (2012), 113001.
[13] I Pallecchi, M Eisterer, A Malagoli, Application potential of Fe-based superconductors, Supercond Sci Technol 28 (11) (2015), 114005.
[14] C Yao, Y. Ma, Recent breakthrough development in iron-based superconducting wires for practical applications, Supercond Sci Technol 32 (2) (2019), 023002.
[15] H Huang, C Yao, C Dong, High transport current superconductivity in powder-in-tube $Ba_{0.6}K_{0.4}Fe_2As_2$ tapes at 27 T, Supercond Sci Technol 31 (1) (2018), 015017.
[16] H Lin, C Yao, X Zhang, Hot pressing to enhance the transport J_c of $Sr_{0.6}K_{0.4}Fe_2As_2$ superconducting tapes, Sci Rep 4 (2014) 6944.
[17] X Zhang, C Yao, H Lin, Realization of practical level current densities in $Sr_{0.6}K_{0.4}Fe_2As_2$ tape conductors for high-field applications, Appl Phys Lett 104 (20) (2014), 202601.
[18] Z Gao, K Togano, Y Zhang, High transport J_c in stainless steel/Ag-Sn double sheathed Ba122 tapes, Supercond Sci Technol 30 (9) (2017), 095012.
[19] C Yao, Y Ma, X Zhang, Fabrication and transport properties of $Sr_{0.6}K_{0.4}Fe_2As_2$ multifilamentary superconducting wires, Appl Phys Lett 102 (8) (2013), 082602.
[20] C Dong, Y Zhu, S Liu, Thermal conductivity of composite multi-filamentary iron-based superconducting tapes, Supercond Sci Technol 33 (7) (2020), 075010.
[21] JD Weiss, C Tarantini, J Jiang, High intergrain critical current density in fine-grain $(Ba_{0.6}K_{0.4})Fe_2As_2$ wires and bulks, Nat Mater 11 (8) (2012) 682–685.
[22] S Liu, K Lin, C Yao, Transport current density at temperatures up to 25K of Cu/Ag composite sheathed 122-type tapes and wires, Supercond Sci Technol 30 (11) (2017), 115007.

[23] S Liu, Z Cheng, C Yao, High critical current density in Cu/Ag composited sheathed $Ba_{0.6}K_{0.4}Fe_2As_2$ tapes prepared via hot isostatic pressing, Supercond Sci Technol 32 (4) (2019), 044007.
[24] T Tamegai, T Suwa, S Pyon, Present status of PIT round wires of 122-type iron-based superconductors, IOP Conf Ser: Mater Sci Eng 279 (2017), 012028.
[25] F Liu, C Yao, H Liu, Observation of reversible critical current performance under large compressive strain in $Sr_{0.6}K_{0.4}Fe_2As_2$ tapes, Supercond Sci Technol 30 (7) (2017), 07LT1.
[26] TTM Palstra, B Batlogg, RB van Dover, Dissipative flux motion in high-temperature superconductors, Phys Rev B 41 (10) (1990) 6621–6632.
[27] PC Canfield, SL Bud'ko, DK Finnemore, An overview of the basic physical properties of MgB_2, Physica C 385 (1-2) (2003) 1–7.
[28] H Yang, H Luo, Z Wang, Fishtail effect and the vortex phase diagram of single crystal $Ba_{0.6}K_{0.4}Fe_2As_2$, Appl Phys Lett 93 (14) (2008) 3.
[29] H Huang, C Yao, Y Zhu, Influences of Tape Thickness on the Properties of Ag-Sheathed $Sr_{1-x}K_xFe_2As_2$ Superconducting Tapes, IEEE Trans Appl Supercond 28 (4) (2018), 6900105.
[30] G Xu, X Zhang, C Yao, Effects of different directional rolling on the fabrication of 7-filament $Ba_{1-x}K_xFe_2As_2$ tapes, Physica C 561 (2019) 30–34.
[31] K Togano, Z Gao, A Matsumoto, Fabrication of $(Ba,K)Fe_2As_2$ tapes by ex situ PIT process using Ag-Sn alloy single sheath, Supercond Sci Technol 30 (1) (2016), 015012.